

УДК 532.526.4

UDC 532.526.4

**ТЕОРИЯ ТУРБУЛЕНТНОСТИ И  
МОДЕЛИРОВАНИЕ ТУРБУЛЕНТНОГО  
ПЕРЕНОСА В АТМОСФЕРЕ  
ЧАСТЬ 3**

**THEORY OF TURBULENCE AND  
SIMULATION OF TURBULENT TRANSPORT  
IN THE ATMOSPHERE  
PART 3**

Трунев Александр Петрович  
к. ф.-м. н., Ph.D.  
Директор, A&E Trounev IT Consulting, Торонто,  
Канада

Alexander Trunev  
Ph.D.  
Director, A&E Trounev IT Consulting, Toronto,  
Canada

В работе представлена полностью замкнутая модель турбулентного пограничного слоя, полученная из уравнения Навье-Стокса. Фундаментальные константы пристенной турбулентности, включая постоянную Кармана, определены из теории. Эта модель была развита для ускоренного и неизотермического пограничного слоя над шероховатой поверхностью

The completely closed model of wall turbulence was derived directly from the Navier-Stokes equation. The fundamental constants of wall turbulence including the Karman constant have been calculated within a theory. This model has been developed also for the accelerated and non-isothermal turbulent boundary layer flows over rough surface

Ключевые слова: ТУРБУЛЕНТНЫЙ ПЕРЕНОС, УСКОРЕННЫЕ ТЕЧЕНИЯ, ПОГРАНИЧНЫЙ СЛОЙ, ШЕРОХОВАТАЯ ПОВЕРХНОСТЬ, ПРИЗЕМНЫЙ СЛОЙ АТМОСФЕРЫ

Keywords: TURBULENT TRANSPORT, ACCELERATED FLOW, BOUNDARY LAYER, ROUGH SURFACE, ATMOSPHERIC SURFACE LAYER

**3 Model of turbulent flows over rough surface**

**3.1 Empirical models of turbulent flow over rough surfaces**

The study of the rough wall turbulence is important in fluid mechanics, in the atmosphere and ocean and in engineering flows [1-74]. The roughness effect on the turbulent boundary layer have been considered and summarised by Nikuradse [75] Schlichting [61,76], Bettermann [77], Millionschikov [78], Dvorak [79], Dirling [80], Simpson [81], Dalle Donne & Meyer [82] and other.

Nikuradse [75] established (for sand-roughened pipes) that if the roughness height significantly exceeds the viscous sublayer thickness, then the mean velocity profile can be described by the logarithmic function:

$$\frac{U}{u_t} = \frac{1}{k} \ln \frac{z}{k_s} + c_s \tag{3.1}$$

where  $u_t$  is the friction velocity,  $u_t = \sqrt{t / r}$ ,  $t$  is the wall shear stress,  $r$  is the fluid density,  $z$  is the distance from the wall - see Figure 3.1,  $k_s$  is the characteristic scale of the sand roughness,  $k, c_s$  are empirical values. Nikuradse found that  $k = 0.4, c_s = 8.5$  for the completely rough regime. He compared the mean velocity profile (3.1) with the law of the wall, derived him before in 1932 for turbulent flows in smooth pipes, as follows

$$\frac{U}{u_t} = \frac{1}{k} \ln \frac{u_t z}{n} + c_0 - \frac{\Delta U}{u_t} \tag{3.2}$$

$n$  is the kinematic viscosity,  $k = 0.4$ ,  $c_0 = 5.5$  are the logarithmic profile constants for the hydraulically smooth surface.  $\Delta U$  is the shift of the mean velocity logarithmic profile which can be defined for the turbulent boundary layer over a rough surface as

$$\frac{\Delta U}{u_t} = \frac{1}{k} \ln \frac{u_t k_s}{n} + D_s \quad (3.3)$$

$D_s \approx -3.0$  for the completely rough regime. Nikuradse has shown that the dimensionless roughness height parameter  $k_s^+ = u_t k_s / n$  can be used as an indicator of the rough wall turbulence regime. He proposed to consider three typical cases:

- § the hydraulically smooth wall for  $0 < k_s^+ \leq 5$ ,  $\Delta U = 0$ ;
- § the transitionally rough regime for  $5 < k_s^+ < 70$ ,  $D_s$  varies with  $k_s^+$ ;
- § the completely rough regime for  $k_s^+ \geq 70$ ,  $D_s \approx -3.0$ .

Thus, the sand-roughened wall turbulence depends on the dimensionless roughness height (roughness Reynolds number)  $k_s^+$  as have been established by Nikuradse.

Schlichting [76], used the Nikuradze's data base and his own experimental results obtained in the water tunnel of rectangular cross section with the upper rough wall, proposed the new form of the equation (3.1) which is well counted the roughness effect on the turbulent boundary layer by means of the effective wall location ( $\Delta z$ ) and the equivalent sand roughness parameter  $k_{es}$ . With these parameters the mean velocity profile in the turbulent flow over an arbitrary rough surface can be written in the Nikuradze's form (3.1) as follows:

$$\frac{U}{u_t} = \frac{1}{k} \ln \frac{z_1}{k_{es}} + c_s \quad (3.4)$$

where  $z_1 = z - \Delta z$  (see Figure 3.1). The effective wall location was defined by Schlichting as the mean height of the roughness elements (the location of a "smooth wall that replaces the rough wall in such a manner as to keep the fluid volume the same"). The value  $k_{es}$  has been measured by Schlichting for the several types of the roughness elements with various shapes, sizes and spacing.

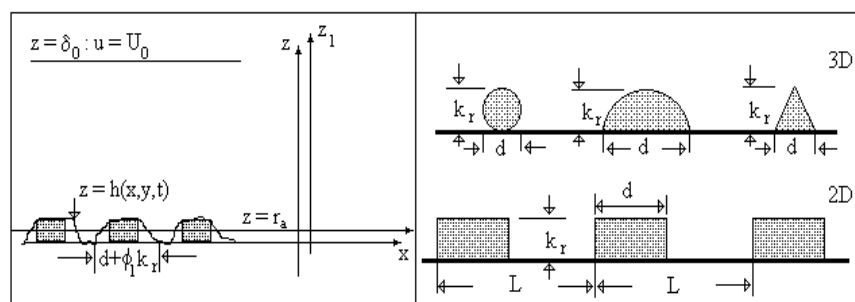


Figure 3.1: The scheme of the turbulent flow over a rough surface (left) and the roughness element geometry (right): spheres, spherical segments, conical elements (3D) and transverse rectangular rods (2D)

The Schlichting's experiment was re-evaluated by Coleman *et. al.* [83] and they noticed that some Schlichting's data have been obtained in the transitional rough regime.

Clauser [84] has shown that the shift of the mean velocity profile can be written as

$$\frac{\Delta U}{u_t} = \frac{1}{k} \ln \frac{u_t k_r}{n} + D$$

where  $k_r$  is the characteristic scale of roughness elements and  $D$  must be some function of the roughness geometrical parameters. Hence the equivalent sand roughness parameter  $k_{es} = k_r \exp[k(D - D_s)]$ , where  $D_s \approx -3.0$  for sand roughness.

Bettermann [77] discovered that  $D$  is the function of the roughness elements spacing. He introduced the roughness density parameter for roughness composed of the transverse square bars as the pitch-to-height ratio,  $\Lambda_B = L / k_r$  - see Figure 3.1. Bettermann found that in the range  $1 \leq \Lambda_B \leq 5$  the variations of  $D$  with the roughness density can be specified by

$$D = 12.25 \ln \Lambda_B - 17.35$$

As has been demonstrated by Dvorak [79], the rough wall effect well correlated with the roughness density parameter defined as pitch-to-width ratio or the ratio of total surface area to roughness area,  $\Lambda_s = L / d$ . Dvorak developed the Bettermann's model in the range  $4.68 \leq \Lambda_s \leq 10^2$ , used the data of Schlichting and other researches, as follows:

$$D = \begin{cases} 12.25 \ln \Lambda_s - 17.35, & 1 \leq \Lambda_s \leq 4.68 \\ -2.85 \ln \Lambda_s + 5.95, & \Lambda_s > 4.68 \end{cases} \quad (3.5)$$

Simpson [81] introduced the roughness density parameter in the case of three-dimensional (3D) roughness as  $\Lambda_s^* = (N_s A_F)^{-1}$  where  $N_s$  is the number of

significant roughness elements per unit area,  $A_f$  is the average frontal area of the significant roughness elements. He suggested the general interpretation of the Bettermann-Dvorak correlation (3.5): two branches (3.5) exist depending on the formation or absence of transverse vortices between roughness elements. Simpson also showed that the shape of the element is an important parameter.

The model been reported by Dirling [80] and verified by Grabow & White [85], takes into consideration the roughness elements shape parameters. The Dirling's density parameter is defined as  $\Lambda_D = (L/k_r)(A_w/A_f)^{4/3}$  where  $A_w$  is "the windward wetted surface area". In a case of two-dimensional (2D) roughness the Dirling's parameter leads to the Bettermann's roughness density parameter. As it was shown by Sigal & Danberg [86] the shape parameters effect can be described by the similar correlation such the equation (3.5) and that  $D = 2.2$  for the two-dimensional roughness in the range  $4.89 \leq \Lambda_s \leq 13.25$ . They also underlined that the correlation for 2D roughness elements is not the same as for 3D elements. On the other hand, Kind & Lawrysyn [87] confirmed that the Bettermann-Dvorak function  $D(\Lambda_s)$  in the form (3.5) can be successfully used for the correlation of experimental data in the aerodynamic experiments with the natural hoar-frost roughness.

Dalle Donne & Meyer [82] correlated their data and those of previously researches (data bases [88-105] considered below) used the roughness density parameter  $\Lambda_D^* = (L-d)/k_r$ . They developed the empirical model which can be applied to the turbulent flows in the annuli and tubes with inner surface roughened by rectangular ribs.

The roughness density parameter entered by Dalle Donne & Meyer [82] in case of 2D roughness elements can be transformed as follows

$$\Lambda_D^* = (L-d)/k_r = (d/k_r)(\Lambda_s - 1)$$

With this parameter the experimental data of Dalle Donne & Meyer [82] and other sources [88-105] summarized in Table 3.1 can be described by equations:

$$D(\Lambda_D^*) = c_0 + (2 + 7/\Lambda_D^*) \lg \frac{k_r}{d} - R, \tag{3.6}$$

$$R = \begin{cases} 9.3(\Lambda_D^*)^{-0.73}, & 1 \leq \Lambda_D^* \leq 6.3 \\ 1.04(\Lambda_D^*)^{0.46}, & 6.3 \leq \Lambda_D^* \leq 160 \end{cases}$$

This correlation has been derived by Dalle Donne & Meyer [82] for the range of the experimental data parameters  $0.086 \leq k_r/d \leq 5.0$  and  $1.85 \leq \Lambda_s \leq 980$ . Therefore the rough surface effect depends on two roughness parameters  $k_r/d$  and  $\Lambda_D^*$ . Thus there is no any "universal" parameter for 2D roughness elements in the common case. But the experimental data with various  $k_r/d$  can be plotted together as the graph of the function

$$D_1(\Lambda_D^*) = D(\Lambda_D^*) - (2 + 7 / \Lambda_D^*) \lg(k_r / d).$$

Table 3.1. Geometrical characteristic of 2D roughness investigated by various authors

Authors	Year	Geometry	$L / d$	$k_r / d$	Symbol
Möbius	1940	Tube	10.0-29.22	0.3-2.20	3
Chu & Streeter	1949	Tube	1.95-7.57	0.93	4
Sams	1952	Tube	2.0-2.3	0.88-1.37	9
Nunner	1956	Tube	16.36	0.8	16
Koch	1958	Tube	9.8-980	1.0-5.0	5
Fedynskii	1959	Annulus	6.67-16.7	1.0	10
Draycott & Lawther	1961	Annulus	2.0	1.0	2
Skupinski	1961	Annulus	2.0-41.0	1.0	6
		Tube	22.2-133.4	2.0	
Savage & Myers	1963	Tube	3.66-43.72	1.33-2.67	13
Perry & Joubert	1963	Wind tunnel	4.0	1.0	19
Sheriff, Gumley & France	1963	Annulus	2.0-10.0	1.0	14
Gargaud & Paumard	1964	Tube	1.8-16.0	1.0-1.67	1
		Annulus	10.0-16.0	1.0	
Bettermann	1966	Wind tunnel	2.65-4.18	1.0	20
Massey	1966	Annulus	7.53-30.15	1.06	15
Kjellström & Larson	1967	Annulus	2.02-38.52	0.086-4.08	12
Fuerstein & Rampf	1969	Annulus	2.91-25.04	0.42-2.50	8
Lawn & Hamlin	1969	Annulus	7.61	1.0	17
Watson	1970	Annulus	6.49-7.22	1.0	11
Stephens	1970	Annulus	7.20	1.0	18
Webb, Eckert & Goldstein	1971	Tube	9.70-77.63	0.97-3.88	7
Antonia & Luxton	1971	Wind tunnel	4.0	1.0	21
Antonia & Wood	1975	Wind tunnel	2.0	1.0	22
Dalle Donne & Meyer	1977	Annulus	4.08-61.5	0.25-2.0	24
Pineau, Nguyen, Dickinson & Belanger	1987	Wind tunnel	4.0	1.0	23

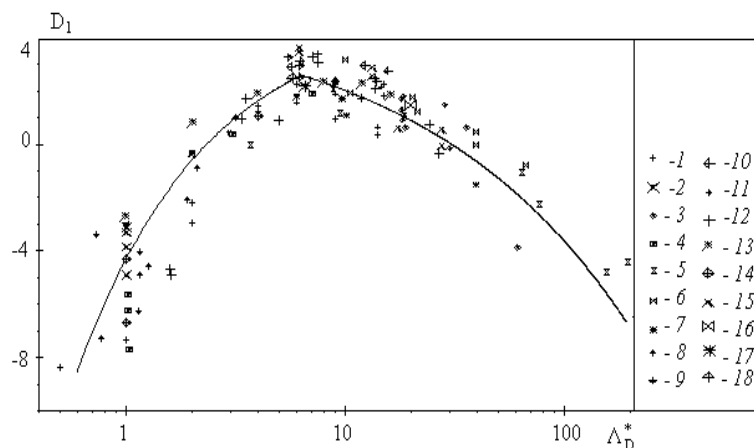


Figure 3.2: The rough surface effect on the turbulent flow: 2D roughness elements data [88-105], the solid line is calculated on the model of Dalle Donne & Meyer [82]

Figure 3.2 demonstrates  $D_1(\Lambda_D^*)$  calculated according to (3.6) - solid line (I) and the experimental data found for 2D roughness elements by various authors listed in Table 3.1 (the corrected and reduced data or  $R(\infty)_{01}$  from Table 2 of Dalle Donne & Meyer [82] has been used as long as correlation (3.6) was proposed for this values). The symbols description is given in the right part of Figure 3.2 and Table 3.1. As Figure 3.2 shows the correlation is good for the middle and high value of the roughness density parameter, but for  $\Lambda_D^* \approx 1$  the scatter of the points is rather large and can't be explained by the experimental technique differences only. The empirical model [82] can't explain the experimental behaviour of the mean velocity shift with a roughness density, which can be found out only by comparison of large number of the data, obtained by various authors [75-77, 81-83, 87-109].

Osaka & Mochizuki [110] examined d-type rough wall boundary layer in a transitionally and a fully rough regime. They have shown that in a transitionally rough regime the mean velocity logarithmic profile is confirmed and that the Karman constant has the same value as for the hydraulically smooth wall flow.

The mean velocity logarithmic profile widely used in the atmospheric turbulence research is given by (see [18-20, 25, 111-113]):

$$\frac{U}{u_t} = \frac{1}{k} \ln \frac{z - z_d}{z_0}$$

where  $z_d$  is the displacement height,  $z_0$  is the roughness length. Note that  $z_d$  and  $z_0$  are considered often as some adjustment parameters chosen for the best correlation of the local wind profile in the neutral stratified flow with the logarithmic profile. The model of the displacement height has been considered by

Jackson [112]. The classification of the experimentally determined roughness length for various terrain types was given by Wieringa [113].

### 3.2 Model of wall roughness effect on turbulent flow

The effective wall location was defined by Schlichting [76] as the mean height of the roughness elements and in the mathematical form can be written as:

$$\Delta z = r_a = \frac{1}{L_x L_y} \iint_{\Delta x \Delta y} r(x, y) dx dy \quad (3.7)$$

where  $z = r(x, y)$  is the relief of the rough surface - see Figure 3.1,  $L_x, L_y$  are the rough wall scales in the  $x, y$  directions,  $\Delta x \Delta y = L_x L_y$ .

In a case of two dimensional roughness considered by Dvorak [79] and Simpson [81] the roughness density parameter depends on the width and pitch of roughness elements (see Figure 3.1):  $\Lambda_s = L/d$ . The mean roughness height depends on the height of roughness elements as  $r_a = ak_r / \Lambda_s$ , where  $a$  is the numerical constant which equals to unity in this case. Using the Bettermann-Dvorak's equation (3.5) in the rang  $4.68 \leq \Lambda_s \leq 10^2$  the shift of the mean velocity can be presented as a function of the mean roughness height, thus we have

$$\begin{aligned} \frac{\Delta U}{u_t} = \frac{1}{k} \ln \frac{u_t k_r}{n} + D &\approx 2.5 \ln \frac{u_t k_r}{n \Lambda_s} - 0.35 \ln \Lambda_s + 5.95 = \\ &= 2.5 \ln \frac{u_t r_a}{n} - 0.35 \ln \Lambda_s + 5.95 \end{aligned}$$

In this approach the mean velocity profile in the turbulent flow over a rough surface can be rewritten as follows

$$\frac{U}{u_t} = \frac{1}{k} \ln \frac{z_1}{r_a} + 0.35 \ln \Lambda_s - 0.45$$

If we redefined the main roughness scale then the mean velocity profile takes the form which widely used in the atmosphere research:

$$\frac{U}{u_t} = \frac{1}{k} \ln \frac{z_1}{r_0} \quad (3.8)$$

where  $\ln r_0 = \ln r_a - 0.35k \ln \Lambda_s + 0.45k \approx \ln r_a - 0.14 \ln \Lambda_s + 0.18$ . Practically  $r_0 \approx r_a$  for  $\Lambda_s = 5$  and  $r_0 \approx 0.63r_a$  for  $\Lambda_s = 100$ . Hence, the logarithmic profile mainly depends on the mean height of the roughness elements in this range of the roughness density.

Let us consider the random function defined as

$$\tilde{u}(z_1 / r) = \frac{u_t}{k} \ln \frac{z_1}{r} \tag{3.9}$$

where  $r$  is the random parameter with the mean value given by

$$r_a = \int_0^\infty r f_s(r) dr$$

here  $f_s = f_s(r)$  is the density of a probability distribution function (roughness statistic function) normalised on unity:

$$\int_0^\infty f_s(r) dr = 1$$

Both parts of equation (3.9) can be averaged with this function as follows

$$U(z_1) = \int_0^\infty \tilde{u}(z_1 / r) f_s(r) dr = \frac{u_t}{k} \int_0^\infty (\ln z_1 - \ln r) f_s(r) dr = \frac{u_t}{k} \ln \frac{z_1}{r_0}$$

where  $\ln r_0 = \int_0^\infty \ln(r) f_s(r) dr$ . With this result the mean-squared-value of the velocity fluctuations can be calculated as

$$d\tilde{u}^2 = \int_0^\infty (\tilde{u} - U)^2 f_s(r) dr = \frac{u_t^2}{k^2} \int_0^\infty (\ln r - \ln r_0)^2 f_s(r) dr$$

Therefore we have

$$d\tilde{u}^2 = \frac{u_t^2}{k^2} \left( \langle \ln^2 r \rangle - \ln^2 r_0 \right)$$

Thus, the random function  $\tilde{u}(z_1 / r)$  can be used for the mean velocity calculation as well as for the mean-squared-value of the velocity fluctuations modeling. Our main idea is that the random function  $\tilde{u}(z_1 / r)$  can be calculated on the basis of a solution of the Navier-Stokes equation due to the *surface layer transformation*

$$\tilde{u}(z_1 / r) = \lim_{dV \rightarrow dV_s} \frac{1}{dV} \int u(x, y, h_1) dx dy dz \tag{3.10}$$

where  $h_1 = z_1 / r(x, y)$  is fixed over the integrated region,  $h_1 = z_1 / r = const$ ,  $dV$  is an arbitrary volume put in  $dV = L_x L_y dz$  and containing  $dV_s$  as a whole,  $dV_s$  is the subregion in which altitude of the rough surface  $r(x, y)$  varies in limits from  $r$  up to  $r + dr$ , hence by definition  $dV_s = dV f_s(r) dr$ .

Note, that the surface layer transformation is only a kind of averaging procedure which conserves the function properties across a boundary layer. The Navier-Stokes equation can be averaged with the surface layer transformation (3.10) instead the normal Reynolds averaging method to derive then the equation for the random amplitude  $\tilde{u}(z_1 / r)$ . Unfortunately it's impossible to use this

method in the simple form (3.10), because, for example, in the case of a smooth flat plate  $r = 0$ .

Therefore we suppose that there is a surface  $z = h(x, y, t)$  (the dynamic roughness surface) inside the flow domain which can be used for modelling the rough surface effect on the turbulent flow. Without any limits we can choose a surface  $z = h(x, y, t)$  close to the wall surface  $z = r(x, y)$ , but not equal to  $r(x, y)$ .

Let  $h(x, y, t) = r(x, y) + h_r(x, y, t)$ , where  $h_r(x, y, t)$  is the height of the viscous sublayer over the rough surface. In the turbulent flow the surface  $z = h(x, y, t)$  can be described by random continuous parameters  $h, h_t, h_x, h_y$  characterised the height, velocity and inclination of the surface elements. Let's define the subregion  $dV_s$  in which the local height of the rough surface  $r(x, y)$  varies in limits from  $r$  up to  $r + dr$  and parameters of the surface  $z = h(x, y, t)$  in limits from  $h$  up to  $h + dh$ , from  $h_t$  up to  $h_t + dh_t$ , from  $h_x$  up to  $h_x + dh_x$ , from  $h_y$  up to  $h_y + dh_y$ , thus

$$dV_s = dV f_s(r, h, h_x, h_y, h_t) dr dh dh_x dh_y dh_t,$$

where  $f_s = f_s(r, h, h_x, h_y, h_t)$  is the multiple density of a probability distribution function. Therefore in common case the surface layer transformation can be written as follows (instead of eq. (2.1) or (3.10))

$$\tilde{\mathbf{u}}(z_1 / h, t, r, h, h_x, h_y, h_t) = \lim_{dV \rightarrow dV_s} \frac{1}{dV} \int_{dV} \mathbf{u}(x, y, h, t) dx dy dz$$

where  $h = z_1 / h(x, y, t)$  is fixed over the region of integration,  $h = z_1 / h = const$ ,  $dV$  is an arbitrary volume put in  $dV = L_x L_y dz$  and containing  $dV_s$  as a whole.

Here again we have the starting point of the theory of turbulence explained in second chapter. On this way we have lost the simplicity of transformation (3.10), as there is an unknown dynamic roughness function  $h = h(x, y, t)$  in transformation (2.1).

The additive dynamic roughness surface model considered above is given by

$$h(x, y, t) = r(x, y) + h_r(x, y, t)$$

where  $h_r(x, y, t)$  is the height of the viscous sublayer over the rough surface. Averaged this equation over a large area  $\Delta x \Delta y = L_x L_y$  we have:  $\bar{h} = r_a + \bar{h}_r$ ,  $\bar{h}_t = \bar{h}_{rt}$ , where  $r_a$  is the mean roughness height, i.e.

$$r_a = \frac{1}{L_x L_y} \iint_{\Delta x \Delta y} r(x, y) dx dy$$

After replacing of the origin of the coordinate system in the new position  $z \rightarrow z - r_a$  the dynamic roughness equation can be written as:

$$h_1(x, y, t) = r(x, y) - r_a + h_r(x, y, t) \tag{3.11}$$

where  $\bar{h}_1 = \bar{h}_r, \bar{h}_{1r} = \bar{h}_{rr}$ . Thus, we can imagine the smooth wall located at  $z = r_a$  as it was defined by Schlichting [76] and the dynamic roughness surface with the dynamic roughness parameters given by (3.11). For this problem we should suggest that  $h_1 > 0$ .

Note that the fluid flow near the plate surface  $z = r_a$  is a typical heterogeneous flow included two parts: the roughness rigid elements part  $S_a = S_a(r_a)$  and the fluid flow part equals to  $\Delta S - S_a$ , where  $\Delta S = L_x L_y$ . Put  $\Lambda_a = \Delta S / S_a(r_a)$  is the ratio of the whole area  $\Delta S = L_x L_y$  to the roughness area  $S_a = S_a(r_a)$  at  $z = r_a$ . The roughness density parameter proposed by Dvorak [79] is given by  $\Lambda_s = \Delta S / S$ , where  $S$  is the total roughness area. Since  $r_a = ak_r / \Lambda_s$ , so  $\Lambda_a = \Lambda_a(r_a)$  can be considered as a function of the Dvorak's roughness parameter:  $\Lambda_a = \Lambda_a(\Lambda_s)$ . For the roughness elements considered by Bettermann [77], Schlichting [76] and Coleman *et. al.* [83] this function can be calculated in the closure form.

For the roughness compounds by the spherical uniform elements  $r_a = 2k_r / 3\Lambda_s$ ,  $S_a(r_a) = S[1 - (1 - 2r_a / k_r)^2]$ , hence

$$\frac{1}{\Lambda_a} = \frac{8}{3\Lambda_s^2} \left( 1 - \frac{2}{3\Lambda_s} \right) \tag{3.12,a}$$

In the case of the surface roughened by spherical segments (Figure 3.1) we have:  $r_a = k_r(3 + k_r^2 / r^2) / 6\Lambda_s$ ,  $S_a(r_a) = S(1 + r_a k_r / r^2)(1 - r_a / k_r)$ , therefore

$$\frac{1}{\Lambda_a} = \frac{S_a(r_a)}{\Delta S} = \frac{1}{\Lambda_s} \left( 1 - \frac{3 + e}{6\Lambda_s} \right) \left( 1 + \frac{e(3 + e)}{6\Lambda_s} \right) \tag{3.12,b}$$

where,  $e = k_r^2 / r^2$ .

In the case of the surface with conical uniform elements we have

$S_a(r_a) = S(1 - r_a / k_r)^2$ ,  $r_a = k_r / 3\Lambda_s$ , thus

$$\frac{1}{\Lambda_a} = \frac{1}{\Lambda_s} \left( 1 - \frac{1}{3\Lambda_s} \right)^2 \tag{3.12,c}$$

In the case of two dimensional roughness as it has been considered by Bettermann [77], Dvorak [79] and Dalle Donne & Meyer [82]  $\Lambda_a = \Lambda_a(r_a)$  depends only on the roughness elements width and pitch (see Figure 3.1):

$$\Lambda_a = \Lambda_s = L / d \tag{3.12,d}$$

The mean liquid surface between the roughness elements at  $z = r_a$  equal to  $(1 - 1/\Lambda_a)\Delta S$ , therefore the mean fluid density  $\bar{r} = (1 - 1/\Lambda_a)r$  (note, that in the real case additionally some liquid volume can be excluded from the mean flow, hence it can be  $\bar{r} = (1 - f/\Lambda_a)r$  where  $f \geq 1$  is the shape parameter counted for instance the liquid involved in the viscous sublayer around the roughness elements). The mean dynamic viscosity is defined as

$$\bar{m} = \bar{r}n = (1 - 1/\Lambda_a)m .$$

Thus,  $\Lambda_a = \Lambda_a(r_a)$  is the important parameter for the rough surface effects modelling because the boundary condition for the mean velocity gradient should be given at  $z = r_a$ .

The mean velocity logarithmic profile in the turbulent flow over the rough surface can be derived from (2.27) written in the new coordinate system:

$$\frac{du^+}{dz_1^+} = \frac{\exp(\hat{F}_0 - \hat{F})}{kI^+ \sqrt{1 + (z_1^+ / I^+)^2}}, \quad \hat{F} = -\frac{h_1}{n} \int_0^{h_1} \frac{\tilde{W} dh_1}{1 + n_1^2 h^2} \quad (3.13)$$

where  $z_1 = z - r_a$ ,  $\hat{F}_0 = \lim_{h \rightarrow \infty} \hat{F}(h)$ ,  $h = z_1 / h_1$ ,  $n_1 = \sqrt{h_{1x}^2 + h_{1y}^2}$ .

The boundary condition for the equation (3.13) on the effective smooth wall is given by

$$\bar{m}du / dz_1 = t_a \quad \text{at} \quad z_1^+ = 0 \quad (3.14,a)$$

where  $t_a$  is the effective shear stress applied to the effective smooth wall at  $z = r_a$ . Thus for the dimensionless mean velocity gradient on the effective wall in common case one can propose that

$$\bar{m}du^+ / dz^+ = \bar{m}G_a = mt_a / t_w \quad \text{at} \quad z_1^+ = 0 \quad (3.14,b)$$

As it follows from the mean velocity logarithmic profile in the turbulent flow established by Schlichting (see eq. (3.4)) the dimensionless turbulent length in the first equation (3.13) depends on the roughness parameters and thus can't be defined from an equation similar to eq. (2.24). To define  $I^+$  note, that for the completely rough regime in the classical sense, when  $k_r^+ \gg 1$ , one can suppose that  $\hat{F} \approx \hat{F}_0$ . Then the exact solution of the problem (3.13)-(3.14) can be written as

$$u^+ = \frac{1}{k} \ln \left( kG_a z_1^+ + \sqrt{1 + (kG_a z_1^+)^2} \right) \quad (3.15)$$

But this equation also follows from (38) if we put  $R_t = 0$  in the non-linear model (24), and therefore  $\hat{F} = \hat{F}_0 = 0$ . Hence, in the case of turbulent flow over a rough surface the main turbulent length scale can be defined as  $I^+ = 1/kG_a \neq I_0^+$ , and the second scale of the turbulent velocity equals zero. The mean velocity

logarithmic profile follows from (3.15) at the long distance from the wall. Put  $z_1^+ \gg 1/kG_a$  in (3.15), and then we have

$$u^+ = \frac{1}{k} \ln z_1^+ + c, \text{ with } c = \frac{1}{k} \ln(2kG_a).$$

This equation can be rewritten in the standard form as follows:

$$u^+ = \frac{1}{k} \ln z_1^+ + c_0 - \frac{1}{k} \ln k_r^+ - D(\Lambda_s), \tag{3.16}$$

$$D(\Lambda_s) = c_0 + \frac{1}{k} \ln \frac{1}{2kk_r^+ G_a}$$

where  $c_0 = 5.015$ . Note, that the finale result (3.16) mainly depends on the mean velocity gradient applied to the effective surface at  $z_1^+ = 0$ .

There are two available cases which can be realised in the experimental situation: the roughness elements installed on the absolutely smooth surface and the roughness elements installed on the rough surface. In the first case we suppose that the mean velocity gradient applied to the effective smooth wall is proportional to the velocity gradient over a smooth surface given by the first equation (2.27) for  $z = r_a$ . Used the boundary condition (3.14, b) we have:

$$(1 - f / \Lambda_a) G_a = \frac{b_r \exp[I_0 - I(r_a^+)]}{k r_a^+ \sqrt{1 + (I_0^+ / r_a^+)^2}} \tag{3.17}$$

where the shape parameter  $f \geq 1$  introduced to estimate the frontal and leeward re-circulation zones effect,  $r_a^+ = r_a u_t / n$ ,  $b_r$  is the parameter. Suggested that  $b_r / \sqrt{1 + (I_0^+ / r_a^+)^2} = b_0$  where  $b_0$  is a function of the roughness parameter, we have (for the smooth background surface):

$$(1 - f / \Lambda_a) G_a = \frac{b_0 g}{k r_a^+}, \quad g = \exp[I_0 - I(r_a^+)] \tag{3.18}$$

here  $g$  is the transitional layer parameter. Note, that for the high value of the roughness density parameter may be  $k_r^+ \gg 1$  (completely rough regime in the classical sense), but simultaneously  $r_a^+ = ak_r^+ / \Lambda_s \leq 1$ . Thus we have  $g = 1$  for the completely rough regime that defined only for  $r_a^+ \gg I_0^+$  as it follows from the second equation (3.18). The main turbulent length scale can be estimated from (3.18) as  $I^+ = 1/kG_a = r_a^+ (1 - f / \Lambda_a) / b_0 g$ . Substituted  $G_a$  from (3.18) into the second equation (3.16) finally we have:

$$D(\Lambda_s) = c_0 + \frac{1}{k} \ln \frac{a(1 - f / \Lambda_a)}{2b_0 \Lambda_s} - \frac{\ln g}{k} \tag{3.19}$$

The rough surface effects model (3.19) depends on two parameters  $b_0, f$  chosen from the best correlation with the experimental data. We should underline that  $b_0$  is the friction parameter of the rough surface and  $f$  is the parameter of the mean density of fluid involved in the mean turbulent flow at the level  $z = r_a$ .

In the second case the mean velocity gradient model is the same as (3.19) but we should put  $r_a = ak_r / \Lambda_s + r_g$  where the averaged height of the background roughness is  $r_g$ . Both models have been testified and shown the good agreement with the experimental data.

### 3.3 Modelling of roughness density effect. 3D roughness elements

To test the roughness surface effect model (3.19) the turbulent flow data for 3D roughness elements obtained by Schlichting [76] and re-evaluated by Coleman *et. al.* [83] has been used. The main result reported by Coleman *et. al.* [83] is that some Schlichting's data was obtained probably in the transitionally rough regime. The experimental techniques in Schlichting's [76] and Coleman *et. al.* [83] experiments have been analyzed and it was surmised that Schlichting's data was measured in the fully rough regime but some details of his experimental technique have not been reported.

The computed (1) and experimental data by Schlichting (3) and Coleman *et. al.* (5) are shown in Figure 3.3 for spheres (Fig. 3.3,a), spherical segments (Fig. 3.3,b) and cones (Fig. 3.3,c). The points (4) are computed from the experimental data by Coleman *et. al.* [83] which has been corrected with transitional layer parameter  $g$  calculated on (2.22) as follows  $g = \exp[1.264 - 0.805 \arctan(0.048r_a^+)]$ .

As it shown in Figure 3.3 the transitional layer effect is essential for the plate with roughness in a form of spherical segments (two points with  $k_r^+ = 14; 27$  and consequently  $\Lambda_s = 31.8; 17.9$ ) and conical elements (two points with  $k_r^+ = 55; 211$  and  $\Lambda_s = 31.8; 17.9$  respectively), and relatively small for all data with  $r_a^+ = ak_r^+ / \Lambda_s \geq 16$ , including data for the plate roughened by spheres.

Note, that the experimental data re-evaluated by Coleman *et. al.* [83] is getting closer to the original Schlichting's data after the correction on the transitional layer effect. Therefore it seems to be clear that the data by Coleman *et. al.* [83] is rather based on another experimental technique than the original Schlichting's data [76].

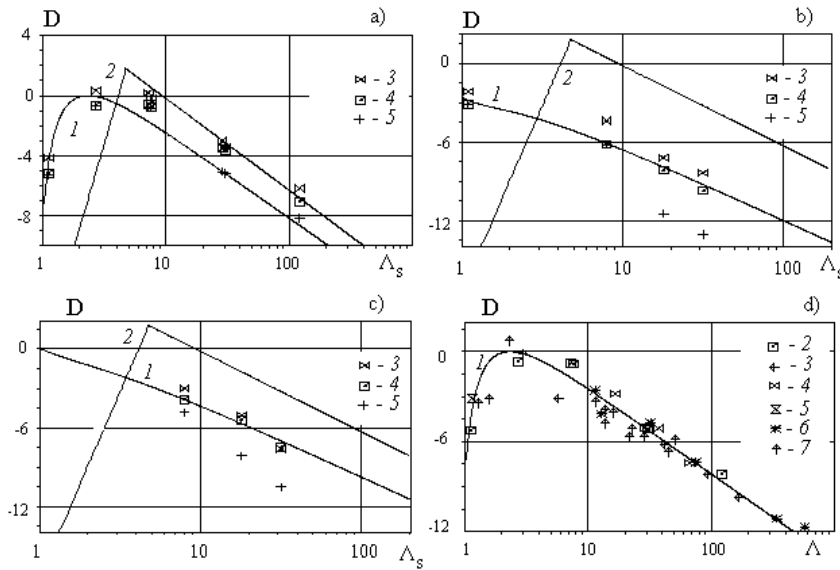


Figure 3.3: Roughness density effect on the turbulent boundary layer for 3D roughness elements: a) spheres; b) spherical segments; c) cones; d) generalised correlation

The corrected data has been used to estimate the parameters  $b_0, f$  in the equation (3.19) which can be written for the completely roughness regime ( $g = 1$ ) as follows

$$D(\Lambda_s) = c_0 + \frac{1}{k} \ln \frac{a(1 - f/\Lambda_a)}{2b_0 \Lambda_s} \quad (3.20)$$

The roughness parameters  $a, \Lambda_a = \Lambda_a(r_a)$  are given by (3.12, a-c) for the spheres, spherical segments and conical elements respectively.

As it has been established in the case of the plate with spheres  $b_0 = 0.65, f = 1.11$  for the data obtained by Coleman *et. al.* [83] (solid line (1) in Figure 3.3,a) and  $b_0 = 0.4, f = 1.25$  for the corrected points. For the roughness elements in the form of spherical segments  $b_0 = 3, f = 1$  (solid line (1), Figure 3.3,b) and for the conical elements  $b_0 = 0.7, f = 1$  - see Figure 3.3,c. For comparison the Bettermann-Dvorak's correlated line (2) also is shown in Figure 3.3.

The magnitude  $b_0$  can be explained in terms of the rough surface drag which has the same value for the spheres and conical elements and much less for the surface with spherical segments. The mean fluid density parameter is  $f \approx 1$  for considered types of roughness elements. Note that in the case of the surface roughened by spheres the function  $D(\Lambda_s)$  has a maximum at  $\Lambda_s \approx 2.35$  (as has

been established in numerical experiments the maximum location depends on the value  $f$  approximately as  $\Lambda_s \approx 2.175f^{2/3}$  for the range  $1 \leq f \leq 2$ ).

The experimental data for the surfaces with spheres, spherical segments or conical elements can be collected together used an "universal" parameter which is different from that proposed by Bettermann [77] Dvorak [79], Dirling [80], Simpson [81], Kind & Lawrysyn [87] and other. This correlation is available for the high roughness density parameter at  $\Lambda_s \gg 1$ , then

$$D(\Lambda_s) \approx c_0 + \frac{1}{k} \ln \frac{a}{2b_0 \Lambda_s}$$

and therefore the "universal" parameter is given by  $\Lambda = b_0 \Lambda_s / a$ . The solid line (1) computed on the equations (3.20) for  $b_0 / a = 1$ ,  $f = 1.11$  is shown in Figure 3.3, d with the corrected experimental data for the rough surfaces with spheres (2), spherical segments (3) and conical elements (4). The classic sand-grain-roughened pipe flow experiment of Nikuradse (1933) with  $D = -3$ ,  $\Lambda_s = 4/p$  is presented by point (5). The hoar-frost roughness data of Kind & Lawrysyn [87] are plotted by points (6). Note, that data of Kind & Lawrysyn [87] has been corrected with transitional layer parameter

$$g = \exp[1.264 - 0.805 \arctan(0.048r_a^+)] / (1 + \Lambda_s r_g / ak_r)$$

where  $r_a = ak_r / \Lambda_s + r_g$ ,  $a = 1/3$ ,  $r_g = k_r f_r$  is the averaged height of the background roughness,  $f_r$  depends on the frost formation and has been calculated for the plate 1-6 of Kind & Lawrysyn [87] as follows  $f_r = .013; .04; .012; .012; .04; .04$ . In this case we have  $b_0 = 0.7$  as for as for conical elements. The experimental data for 3D rounded elements of Simpson (1973) is shown by symbols (7), and for his data  $0.45 \leq b_0 / a \leq 0.55$ .

Thus one can suggest that the rough surface with spheres is the basic case for 3D roughness elements because all data shown in Figure 3.3,d is correlated well with the basic line (1).

Then one can propose the model for  $b_0$  considered this parameter as a function of the width-to-height ratio  $b_0 = b_0(d / k_r)$ . For instance, at  $b_0 / a = 1$  we have the Dvorak's roughness density parameter  $\Lambda = \Lambda_s = \Delta S / S$ . For a linear function  $b_0 = b_0(d / k_r)$  the "universal" parameter is related to that of Bettermann (1966) since in the case of transverse square bars  $S = d$ ,  $a = 1$  and hence  $\Lambda = b_1 L / k_r$ , where  $b_1$  is the numerical value. Another forms of the roughness density parameter [80-81, 85-86] are based on an approximation of function  $b_0 = b_0(d / k_r)$ , dependent on available experimental data and theoretical consideration of the roughness elements drag in turbulent flows.

### 3.4. Modelling of roughness density effect. 2D roughness elements

Using the roughness density parameter model in the form (3.12, d) and suggesting that  $g = 1$  (completely roughness regime) one can write (3.19) for this case as follows

$$D(\Lambda_s) = c_0 + \frac{1}{k} \ln \frac{(1 - f / \Lambda_s)}{2b_0 \Lambda_s} \quad (3.21)$$

For the constant value of the parameters  $b_0, f$  the function  $D(\Lambda_s)$  has a maximum at  $\Lambda_s = 2f$ . This maximum can be defined from the Dalle Donne & Meyer's model (3.6) as  $\Lambda_s = 6.3k_r / d + 1$ , and therefore  $f = (6.3k_r / d + 1) / 2$ . Thus as it follows from the experimental data the shape parameter varies with  $k_r / d$ . To compare the experimental data with the arbitrary value of the shape parameter let us introduce the roughness density parameter in the form  $\Lambda_f = \Lambda_s / f$ , then the roughness surface effect model can be rewritten as

$$D(\Lambda_f) = c_0 + \frac{1}{k} \ln \frac{(1 - 1 / \Lambda_f)}{2b_1 \Lambda_f} - \frac{1}{k} \ln(df / k_r) \quad (3.22)$$

where  $b_1 = b_0 k_r / d$ .

In this model the experimental data for various  $k_r / d$  can be plotted together as the graph of the function

$$D_f(\Lambda_f) = D(\Lambda_f) + 1/k \ln(df / k_r)$$

as well as in the Dalle Donne & Meyer's model (3.6). But as it has been established the shape parameter derived from the model (3.6) isn't a good approximation.

Note that in the common case one can suggest that  $f = 1 + f_1 k_r / d$ , where  $f_1 k_r$  is the total length of the frontal and leeward re-circulation zones. The model (3.6) gives for this parameter an unreasoned result that  $f_1 = 3.15 - d / 2k_r$ . Thus the experimental data of various authors listed in Table 3.1 has been used to find the right form of  $f$  and  $b_0$ . The best correlation for about 130 points is given by

$$f = 1 + f_1 \frac{k_r}{d}, \quad f_1 = \exp(-B^{q_1} \ln B^{1/q_1}), \quad b_0 = b_1 \frac{d}{k_r} \quad (3.23)$$

where  $B = (1 + k_r / d) / \Lambda_s$ ,  $q_1 = 0.625$ ,  $b_1 = 0.12$ .

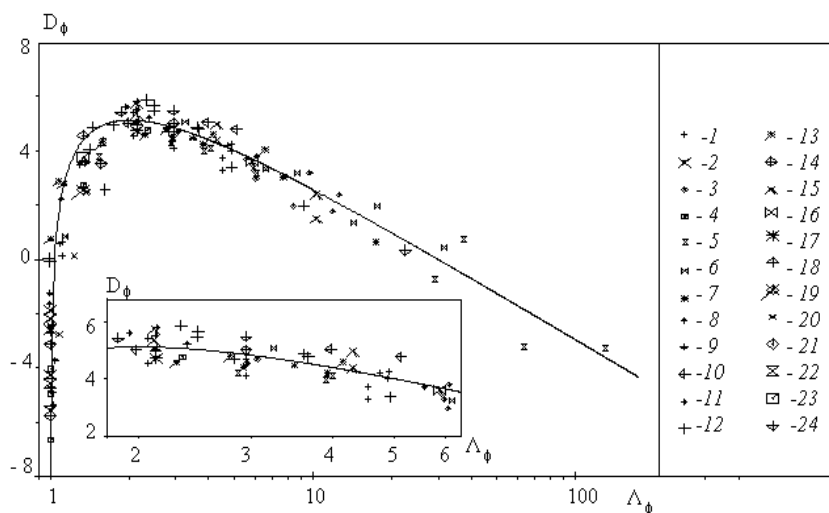


Figure 3.4: The rough surface effect on the turbulent flow: 2D roughness elements data 1-24, the solid line is calculated on (3.22-3.23). The multiply fragment of correlation line is shown in the lower part

Figure 3.4 shows  $D_f(\Lambda_f)$  calculated on (3.22-3.23) - the solid line (1), and the experimental data 1-24 of various authors listed in Table 3.1 (note, we have used values  $R(\infty)$  from Table 2 of Dalle Donne & Meyer [82] instead of the original data 1-18). The symbols description is given in the right part of Figure 3.4 and in Table 3.1. A fragment of the correlated line is shown in the lower part of Figure 3.4. One can see that the predicted roughness density effect (solid line) is in a good agreement with the main experimental data.

Finally note, that model (3.22-3.23) is derived for the rough surface composed by the transverse rectangular rods and can't be applied to 2D roughness elements of another form without additionally verification.

### 3.5 Model of total length of frontal and leeward re-circulation zones

Analyzing expression (3.22) one can find two singular points:  $\Lambda_f \rightarrow 1$  and  $\Lambda_f \rightarrow \infty$  which correspond to two branches of function  $D_f(\Lambda_f)$ . Dalle Donne & Meyer [82] model (3.6) also has two singular points  $\Lambda_D^* \rightarrow 0$  and  $\Lambda_D^* \rightarrow \infty$ . Taken into account that  $\Lambda_D^* = (d/k_r)(\Lambda_s - 1)$  one can conclude that these two singular points are located at  $\Lambda_s \rightarrow 1$  and  $\Lambda_s \rightarrow \infty$  accordingly. As we can see from the data shown in Figures 3.2 there is probably another singular point at  $\Lambda_D^* \approx 1$ . The data collected around the point at  $\Lambda_D^* \approx 1$  has been obtained mainly for  $k_r/d = 1$ . Thus this point can be at  $\Lambda_s \approx 2$ . But generally speaking what is the physical reason for this point? In Figure 3.5, a the normalised total length of the frontal and leeward re-circulation zones (solid lines) which depends on the Dvorak's roughness density parameter  $f_1 = f_1(\Lambda_s)$  and the mean fluid density (broken line) calculated for  $k_r/d = 0.5; 2; 5$  are shown.

As we can see from Figure 3.5,a the total length has a maximum located in a point  $\Lambda_s^* = \Lambda_s^*(k_r/d)$ . According to this the effective mean fluid density has a minimum which may be less than zero. As it follows from (3.14, b), if  $t_a$  is limited value and  $\bar{m} \rightarrow 0$  then  $G_a \rightarrow \pm\infty$  thus it is a singular point for the function  $D = D(\Lambda_s)$ . Physically it means that the frontal and leeward re-circulation zones have intersection. As it is well known in this case the skimming flow is realised. In the model (3.22)-(3.23) this regime is counted statistically and probably with some error. In any case the data over the point  $\Lambda_d^* \approx 1$  in Figure 3.2 is replaced to the point  $\Lambda_f = 1$  in Figure 3.4. Note that correlated line goes throughout this data better in Figure 3.4 than in Figure 3.2.

An unexpected result has been found out in the numerical experiment that function  $D = D(\Lambda_s)$  has one maximum for  $k_r/d < 1.436$  and two maximum for  $k_r/d \geq 1.436$  as shown by the solid lines 1 in Figure 3.5,b calculated for  $k_r/d = 5$ . This result is very sensitive to the variations of the value  $f_1$ . If  $f_1$  is multiplied by 0.9 then the function  $D = D(\Lambda_s)$  loses the singular point and looks like solid line 2 in Figure 3.5,b. Now we have only experimental data shown in Figure 3.4 which is not sufficient to confirm this result.

A restriction for this model can be established if the length scale  $I^+ = r_a^+(1-f/\Lambda_a)/b_0g$  found out for the rough surface is compared with the main turbulent length scale  $I_0^+$  computed for the boundary layer over a smooth surface as  $I^+ \geq I_0^+$ . It puts the limitation for the normalised mean fluid density as  $(1-f/\Lambda_a) \geq I_0^+b_0/r_a^+ \approx 1/r_a^+$  for 2D roughness considered above. If this restriction is broken then it means that the model (3.22)-(3.23) also can't be used properly. Supposed that in this case  $I^+ = I_0^+$  one can regularise the function  $D = D(\Lambda_s)$  in the singular point shown in Figure 3.5,b.

### 3.6 About efficiency of air pollutants removal

The efficiency of the air pollutants removal from the urban streets depends on several parameters including the emission rate, wind speed and aerodynamic properties of the streets. For the one road system this problem is reduced to the estimation of aerodynamic properties of the street depending on the geometry of ambient buildings [16, 114]. In case of several parallel streets with uniform buildings, the problem mainly is similar to the task about turbulent flows over a rough surface with artificial 2D roughness elements which was considered above.

So, put  $k_r$  is the scale of buildings height,  $L$  is the mean distance between streets,  $l$  is the typical width of roads;  $\tilde{q}$  is the specific emission of a typical vehicle,  $N_i^{\&}$  is the number of vehicles passing through chosen cross-section of a road on the street "i" per fixed time interval. Then, the specific emission on the

street 'i' is determined as  $q^i = \tilde{q} N_i^i / l$ . Note, that  $\tilde{q}$  is the technique characteristic of the vehicle.

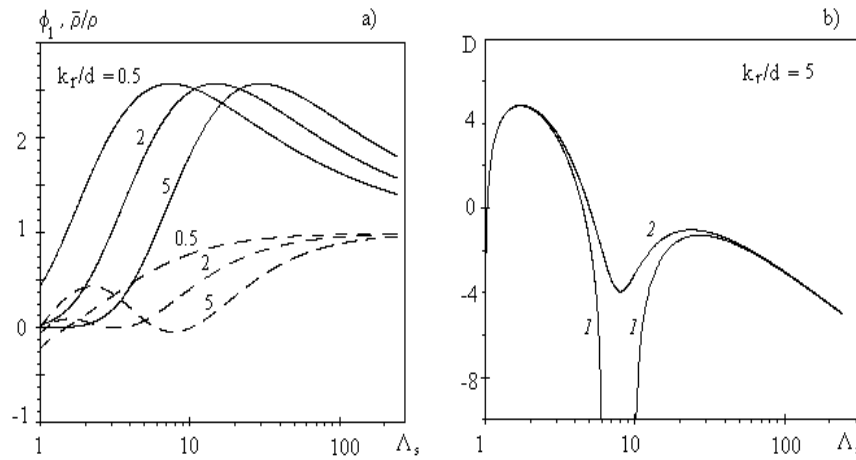


Figure 3.5: a) the normalised total length of the frontal and leeward re-circulation zones (solid lines) versus the Dvorak's roughness density parameter  $f_1 = f_1(\Delta_s)$  and the normalised mean fluid density (broken line) calculated for  $k_r/d = 0.5; 2; 5$ .; b) the roughness density effect on the mean velocity shift  $D = D(\Delta_s)$  at fixed  $k_r/d = 5$ . The solid line 1 is calculated on (3.22)-(3.23), The solid line 2 is calculated also on (3.22)-(3.23), with parameter  $f_1$  decreased on 10%

Assuming that all emitted gases are removed from the street by turbulent flow, one can define the turbulent scale of impurity concentration on the street "i" as:  $C_i^* = q^i / u_*$ . Hence, the impurity concentration near to the road is proportional to the emission rate and inversely proportional to the wind friction velocity. But the turbulent velocity scale in turn depends on a wind velocity on the external boundary of turbulent flow. Using the first equation (3.16) on the level  $z = H$ , one can written the wind velocity in the logarithmic layer

$$\frac{U}{u_*} = \frac{1}{k} \ln \frac{H - z_0}{k_r} + c_0 - D$$

From here the wind friction velocity and turbulent scale of concentration can be defined as follows

$$u_* = U \left( \frac{1}{k} \ln \frac{H - z_0}{k_r} + c_0 - D \right)^{-1}, \quad C_i^* = \frac{q^i}{U} \left( \frac{1}{k} \ln \frac{H - z_0}{k_r} + c_0 - D \right) \quad (3.24)$$

These expressions can be used for an evaluation of efficiency of air pollutants removal from streets depending on the geometric parameters. Setting of the

wind velocity at height  $H = mk_r \gg z_0$ , where  $m$  is the numerical value and simplifying the second expression (3.24), we have:

$$C_i^* = \frac{q^i}{U} \left( \frac{1}{k} \ln m + c_0 - D \right) \tag{3.25}$$

In activities [41-42] and some other, it is offered to measure the wind velocity in urban environment at the level  $H = k_r$ , therefore for  $m = 1$ , but it isn't right, because the mean velocity profile is not homogeneous on this height.

Thus, the problem about efficiency of air pollutants removal from the streets is reduced to that to minimise the expression (3.25). If the parameter of emission, wind velocity and the wind speed parameter  $m$  are given, then a minimum of the dynamic concentration is reached at a maximum of  $D(\Lambda_s)$ .

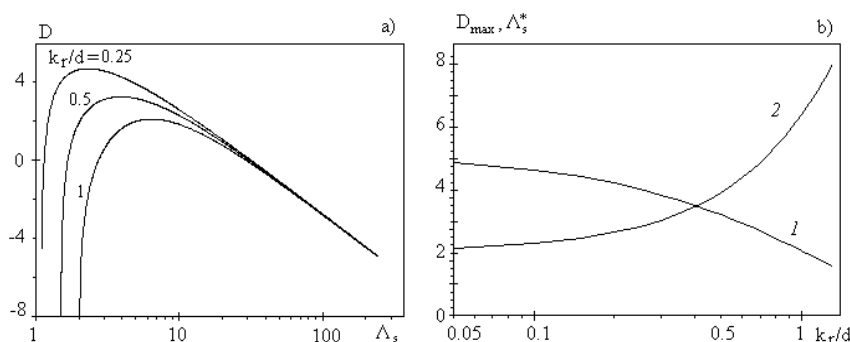


Figure 3.6: a) The shift of the mean velocity logarithmic profile versus parameter of roughness density; b) the maximum of mean velocity logarithmic profile shift vs the roughness elements height to width ratio

The function  $D = D(\Lambda_s)$  computed for the various roughness elements height to width ratio  $k_r / d = 0.25; 0.5; 1$  is shown in Figure 3.6, a. Note that  $D(\Lambda_s)$  has only one maximum for the parameter  $k_r / d$  from the interval  $0 < k_r / d < 1.436$ , thus the problem of minimisation has only one solution. The numerical solution  $D_{\max} = D_{\max}(k_r / d)$  is shown in Figure 3.6, b by the solid line 1. In the interval  $k_r / d \geq 1.436$  the function  $D_{\max} = D_{\max}(k_r / d)$  has two branches, but this solution is not shown. The position of maximum dependent on  $k_r / d$  is shown in Figure 3.6, b by the solid line 2.

Finally note that only the case of the neutral stratified turbulent flow has been considered. The problem about turbulent diffusion in the atmospheric boundary layer with an arbitrary stratification over the region with several streets will be analysed in the subsection 5.2 of Part 5.

Therefore, the model of turbulent boundary layer over rough surface has been given and it has been stated that the profile of a mean velocity in turbulent boundary layer can be described by logarithmic function with the parameters, depending on geometry of elements of roughness. Model application in the case of three-dimension elements of roughness of the type of spheres, spherical segments and cones, as well as in the case of two-dimension elements of roughness of the type rectangular rods, placed on the flat surface with equal step has been considered. The basic parameters of model have been evaluated. Equations, describing summary volume of re-circulating zones and elements resistance to roughness have been obtained. The question about possibility of application the obtained results for modelling the efficiency of city streets ventilation have been considered.

(To be continued)

## References

- [1] Liepmann, H.W., The Rise and Fall of Ideas in Turbulence, *American Scientist*, **67**, pp. 221-228, 1979.
- [2] Amirkhanov, M.M, Lukashina, N.S. & Trunev, A. P., *Natural recreation resources, state of environment and economical and legal status of coastal resorts*, Publishing House "Economics", Moscow, 207 p., 1997 (in Russian).
- [3] Marchuk, G. I., *Mathematical Modelling in the Environmental Problem*, "Nauka", Moscow, 1982 (in Russian).
- [4] Borrell P.M., Borrell P., Cvitas T. & Seiler W., Transport and transformation of pollutants in the troposphere. *Proc. EUROTRAC Symp.*, SPB Academic Publishing, Hague, 1994.
- [5] Jaecker-Voirol A., Lipphardt M., Martin B., Quandalle, Ph., Salles, J., Carissimo, B., Dupont, E., Musson-Genon, L., Riboud, P.M., Aumont, B., Bergametti, G., Bey, I., Toupance, G., A 3D regional scale photochemical air quality model - application to a 3 day summertime episode over Paris, *Air Pollution IV. Monitoring, Simulation and Control*, eds. B. Caussade, H. Power & C.A. Brebbia, Comp. Mech. Pub., Southampton, pp. 175-194, 1996.
- [6] Borrego, C., Coutinho, M., Carvalho, A.C.& Lemos, S., A modelling package for air quality management in Lisbon, *Air Pollution V. Modelling, Monitoring and Management*, eds. H. Power, T. Tirabassi & C.A. Brebbia, CMP, Southampton-Boston, pp. 35-44, 1997.
- [7] Bozo, L.& Baranka, G., Air quality modelling over Budapest, *Air Pollution IV. Monitoring, Simulation and Control*, eds. B. Caussade, H. Power & C.A. Brebbia, Comp. Mech. Pub., Southampton, pp. 31-36, 1996.
- [8] Marchuk, G.I. & Aloyan, A.E., Global Admixture Transport in the Atmosphere, *Proc. Rus. Acad. Sci., Phys. Atmosphere and Ocean*, **31**, pp. 597-606, 1995.
- [9] Moussiopoulos N., Air pollution models as tools to integrate scientific results in environmental policy, *Air Pollution III, Vol.1. Theory and Simulation*, eds. H. Power, N. Moussiopoulos & C.A. Brebbia, Comp. Mech. Publ., Southampton, pp.11-18, 1995.
- [10] Pekar M., *Regional models LPMOD and ASIMD. Algorithms, parametrization and results of application to Pb and Cd in Europe scale for 1990*, EMEP/MSC-E Report 9/96, Aug, 78 p., 1996.
- [11] Carruthers, D.J, Edmunds, H.A., McHugh, C.A., Riches, P.J. & Singles, R.J., ADMS Urban - an integrated air quality modelling system for local government, *Air Pollution V. Modelling, Monitoring and Management*, eds. H. Power, T. Tirabassi & C.A. Brebbia, CMP, Southampton-Boston, pp. 45-58, 1997.
- [12] Ni Riain, C., Fisher, B., Martin, C. J. & Littler J., Flow field and Pollution Dispersion in a Central London Street, *Proc. of the 1st Int. Conf. on Urban Air Quality: Monitoring and Modelling*, ed. R. S. Sokhi, Kluwer Academic Publishers, pp. 299-314, 1998.

- [13] Lukashina, N.S. & Trunev, A. P., *Principles of Recreation Ecology and Natural Economics*, Russian Academy of Sciences, Sochi, 273 p., 1999 (in Russian).
- [14] Lukashina, N.S., Amirkhanov, M.M, Anisimov, V.I. & Trunev, A.P., Tourism and environmental degradation in Sochi, Russia, *Annals of Tourism Research*, **23**, pp. 654-665, 1996.
- [15] Lenhart, L. & Friedrich, R. European emission data with high temporal and spatial resolution, *Air Pollution III Vol.2: Air Pollution Engineering and management*, eds. H. Power, N. Moussiopoulos & C.A. Brebbia. Comp. Mech. Pub., Southampton, pp.285-292, 1995.
- [16] Oke, T.R., Street design and urban canopy layer climate, *Energy and Buildings*, **11**, pp. 103-111, 1988.
- [17] Zilitinkevich, S. Non-local turbulent transport: pollution dispersion aspects of coherent structure of convective flows, *Air Pollution III, Vol.1. Air Pollution Theory and Simulation*, eds. H. Power, N. Moussiopoulos & C.A.Brebbia, Comp. Mech. Publ., Southampton, pp.-53-60, 1995.
- [18] Arya, S. P., *Introduction to Micrometeorology*, Academic Press, San Diego, 307 p., 1988.
- [19] Stull, R. B., *An Introduction to Boundary Layer Meteorology*, Kluwer Academic Publishers, Dordrecht, 666 p., 1988.
- [20] Kaimal, J. C. & Finnigan, J. J., *Atmospheric Boundary Layer Flows: Their Structure and Measurements*, Oxford University Press, 289 p., 1994.
- [21] Monin, A.S. & Obukhov, A.M., Basic Laws of Turbulent Mixing in the Atmospheric surface layer, *Trudy Geofiz. Inst. Akad. Nauk SSSR* **24** (151), pp. 163-187, 1954.
- [22] Monin, A. S., The Atmospheric Boundary Layer, *Ann. Rev. Fluid Mech.*, **22**, 1970.
- [23] Businger, J.A., Wyngaard, J.C., Izumi, Y. & Bradley, E.F. Flux Profile Relationships in the Atmospheric Surface Layer, *J. Atmos. Sciences*, **28**, pp.181-189, 1971.
- [24] Businger, J. A., A Note on the Businger-Dyer Profile, *Boundary-Layer Meteorol.*, **42**, pp. 145–151, 1988.
- [25] Yaglom, A.M., Data on Turbulence Characteristics in the Atmospheric Surface Layer, *Izv. Acad. Sci. USSR, Phys. Atmosphere and Ocean*, **10**, pp. 566-586, 1974.
- [26] Dyer, A. J., A Review of Flux-Profile Relationships, *Boundary-Layer Meteorol.*, **7**, pp. 363–372, 1974.
- [27] Van Ulden, A. & Holtslag, A. A. M., Estimation of Atmospheric Boundary Layer Parameters for Diffusion Applications, *J. Clim. Appl. Meteorol.*, **24**, pp. 1196–1207, 1985.
- [28] Hanjalic, K. & Launder, B. E., A Reynolds Stress Model of Turbulence and its Application to Thin Shear Flows, *J. Fluid Mech*, **52**, pp. 609–638, 1972.
- [29] Rodi, W. Calculation of Stably Stratified Shear-layer Flows with a Buoyancy-extended  $k - \epsilon$  Turbulence Model, *Turbulence and Diffusion in Stable Environments*, ed. J. C. R. Hunt, Clarendon Press, Oxford, pp. 111–143, 1985.
- [30] Mellor, G. L. & Yamada, T. A. Hierarchy of Turbulence Closure Models for Planetary Boundary Layers, *J. Atmos. Sci.*, **31**, pp. 1792–1806, 1974.
- [31] Mellor, G. L. & Yamada, T., Development of a Turbulence Closure Model for Geophysical Fluid Problems, *Rev. Geophys. Space Phys.*, **20**, pp.851–875, 1982.
- [32] Wyngaard, J. C. & Cote, O. R., The Evolution of a Convective Planetary Boundary Layer – a Higher-order-closure Model Study, *Boundary-Layer Meteorol.*, **7**, pp. 289–308, 1974.
- [33] Zeman, O. & Lumley, J. L., Modelling Buoyancy Driven Mixed Layers, *J. Atmos. Sci.*, **33**, pp.1974–1988, 1976.
- [34] Deardorff, J. W. & Willis, G. E., Further Results from a Laboratory Model of the Convective Boundary Layer, *Boundary-Layer Meteorol*, **32**, pp. 205–236, 1985.
- [35] Enger, L., A Higher Order Closure Model Applied to Dispersion in a Convective PBL, *Atmos. Environ.*, **20**, pp. 879–894, 1986.
- [36] Holt, T. & Raman, S., A Review and Comparative Evaluation of Multilevel Boundary Layer Parameterisations for First Order and Turbulent Kinetic Energy Closure Schemes, *Rev. Geophys. Space Phys.*, **26**, pp. 761–780, 1988.
- [37] Danilov, S.D., Koprov, B. M. & Sazonov, L. A., Atmospheric Boundary Layer and the Problem of Its Description (Review), *Proc. Rus. Acad. Sci., Phys. Atmosphere and Ocean*, **31**, pp. 187-204, 1995.
- [38] Hurley, P. J., An Evaluation of Several Turbulence Schemes for the Prediction of Mean and Turbulent Fields in Complex Terrain, *Boundary-Layer Meteorol.*, **83**, pp. 43–73, 1997.

- [39] Reynolds, O., On the dynamically theory of incompressible viscous fluids and the determination of the criterion, *Philos. Trans. R. Soc. London*, **A 186**, 123, 1895.
- [40] Boussinesq, J., Theorie de l'ecoulement tourbillant, *Mem. Pres. Acad. Sci.*, **23**, p. 46, 1877.
- [41] Prandtl, L., Bericht uber untersuchungen zur ausgebildeten turbulenz, *Z. Angew. Math. Mech.*, **5**, pp.136-139, 1925.
- [42] Prandtl, L., Neuere Ergebnisse der Turbulenzforschung, *VDI -Ztschr.*, **77**, 5, p.105, 1933.
- [43] Kolmogorov, A.N., The Equations of Turbulent Motion in an Incompressible Fluid, *Izv. Acad. Sci. USSR, Phys.*, **6**, pp. 56-58, 1942.
- [44] Apsley, D. D. & Castro, I. P., A Limited-Length-Scale-Model for the Neutral and Stable-Stratified Atmospheric Boundary Layer, *Boundary Layer Meteorol.*, **83**, pp. 75-98, 1997.
- [45] Trunev, A. P., Diffuse processed in turbulent boundary layer over rough surface, *Air Pollution III, Vol.1. Theory and Simulation*, eds. H. Power, N. Moussiopoulos & C.A. Brebbia, Comp. Mech. Publ., Southampton, pp. 69-76, 1995.
- [46] Trunev, A. P., Similarity theory and model of turbulent dusty gas flow over large-scale roughness, *Abstr. of Int. Conf. On Urban Air Quality: Monitoring and Modelling*, University of Hertfordshire, Institute of Physics, London, p. 3.8, 1996.
- [47] Trunev, A. P., Similarity theory for turbulent flow over natural rough surface in pressure and temperature gradients, *Air Pollution IV. Monitoring, Simulation and Control*, eds. B. Caussade, H. Power & C.A. Brebbia, Comp. Mech. Pub., Southampton, pp. 275-286, 1996.
- [48] Trunev, A. P., Similarity theory and model of diffusion in turbulent atmosphere at large scales, *Air Pollution V. Modelling, Monitoring and Management*, eds. H. Power, T. Tirabassi & C.A. Brebbia, CMP, Southampton-Boston, pp. 109-118, 1997.
- [49] Klebanoff, P. S., Characteristics of turbulence in a boundary layer with zero pressure gradient, *NACA Tech. Note*, **3178**, 1954.
- [50] Laufer, J., The structure of turbulence in fully developed pipe flow, *NACA Tech. Note*, **2954**, 1954.
- [51] Cebeci, T. & Bradshaw, P., *Physical and Computational Aspects of Convective Heat Transfer*, Springer-Verlag, NY, 1984.
- [52] Cantwell, Brian J., Organized motion in turbulent flow, *Ann. Rev. Fluid Mech.*, **13**, pp. 457-515, 1981.
- [53] Kuroda, A., *Direct Numerical Simulation of Couette-Poiseuille Flows*, Dr. Eng. Thesis, the University of Tokyo, Tokyo, 1990.
- [54] Coleman, G.N., Ferziger, J. R. & Spalart, P. R., A numerical study of the turbulent Ekman layer, *J. Fluid Mech.*, **213**, pp.313-348, 1990.
- [55] Trunev, A. P. & Fomin, V. M., Continual model of impingement erosion, *J. Applied Mech. Tech. Phys.*, **6**, pp. 113-120, 1985.
- [56] Trunev, A. P., *Research of bodies erosion distraction in gas flows with admixture particles*, Ph.D. Thesis, Inst. Theoretical and Appl. Mech., Novosibirsk, 1986.
- [57] Nikolaevskii, V.N., The space averaging in the turbulence theory, *Vortexes and Waves*, ed. V.N. Nikolaevskii, Mir, Moscow, pp. 266-335, 1984 (in Russian).
- [58] Landau, L.D. & Lifshitz, E. M., *Hydrodynamics*, 3<sup>rd</sup> ed., Nauka, Moscow, 1986 (in Russian).
- [59] Pulliam, T. H. & Steger, J. L., Implicit Finite-Difference Simulations of three-dimensional Compressible Flow, *AIAA Journal*, **18**, p. 159, 1980.
- [60] Hirschel, E.H. & Kordulla, W., *Shear Flow in Surface-Oriented Coordinates*, Friedr. Vieweg & Sohn, Wiesbaden, 1986.
- [61] Schlichting, H., *Boundary Layer Theory*, McGraw-Hill, NY, 1960.
- [62] Kutateladze, S.S., *The Wall Turbulence*, Nauka, Novosibirsk, 1973 (in Russian).
- [63] Hairer, E., Norsett, S.P. & Wanner, G., *Solving Ordinary Differential Equations 1. Nonstiff Problems*, Springer-Verlag, Berlin, 1987.
- [64] Cantwell, B. J., Coles, D. E. & Dimotakis, P. E., Structure and entrainment in the plane of symmetry of a turbulent spot, *J. Fluid Mech.*, **87**, pp. 641-672, 1978.
- [65] Van Driest, E.R., On turbulent flow near a wall, *J. Aero. Sci.*, **23**, p.1007, 1956.
- [66] Kuroda, A., Kasagi, N. & Hirata, M., A Direct Numerical Simulation of the Fully Developed Turbulent Channel Flow, *Proc. Int. Symp. on Computational Fluid Dynamics*, Nagoya, pp. 1174-1179, 1989.

- [67] Nagano, Y., Tagawa, M. & Tsuji, T., Effects of Adverse Pressure Gradients on Mean Flows and Turbulence Statistics in a Boundary Layer, *Proc. 8th Symposium on Turbulent Shear Flows*, 1992.
- [68] Nagano, Y., Kasagi, N., Ota, T., Fujita, H., Yoshida, H. & Kumada, M., *Data-Base on Turbulent Heat Transfer*, Department of Mechanical Engineering, Nagoya Institute of Technology, Nagoya, DATA No. FW BL004, 1992.
- [69] Smith, R.W., *Effect of Reynolds Number on the Structure of Turbulent Boundary Layers*, Ph.D. Thesis, Princeton University, Princeton, NJ, 1994.
- [70] Kline, S.J., Reynolds, W.C., Schraub, F.A. & Runstadler P.W., The structure of turbulent boundary layers, *J. Fluid Mech.*, **30**, pp. 741-773, 1967.
- [71] Kriklivy, V.V., Trunev, A.P. & Fomin, V.M., Investigation of two-phase flow in channel with damaging wall, *J. Applied Mech. Tech. Phys.*, **1**, pp. 82-87, 1985.
- [72] Trunev, A. P. & Fomin, V.M., Surface instability during erosion in the gas-particles stream, *J. Applied Mech. Tech. Phys.*, **3**, pp. 78-84, 1986.
- [73] Trunev, A. P., Evolution of the surface relief at sputtering by ionic bombardment, *Interaction of nuclear particles with a rigid body*, Moscow, Vol.1, Part 1, pp. 83-85, 1989.
- [74] Blackwelder, R. F. & Eckelmann, H., Streamwise vortices associated with the bursting phenomena, *J. Fluid Mech.*, **94**, pp. 577-594, 1979.
- [75] Nikuradse, J., Strömungsgesetze in Rauhen Röhren, *ForschHft. Ver. Dt. Ing.*, p. 361, 1933.
- [76] Schlichting, H., Experimentelle Untersuchungen zum Rauheitsproblem, *Ing.-Arch*, **7**(1), pp.1-34, 1936.
- [77] Bettermann, D., Contribution a l'Etude de la Convection Force Turbulente le Long de Plaques Regueuses, *Int. J. Heat and Mass Transfer*, **9**, p. 153, 1966.
- [78] Millionschikov, M.D., *Turbulent flows in the boundary layer and in the tubes*, Nauka, Moscow, 1969 (in Russian).
- [79] Dvorak, F. A., Calculation of Turbulent Boundary Layer on Rough Surface in Pressure Gradient, *AIAA Journal*, **7**, 1969.
- [80] Dirling, R.B., Jr., A Method for Computing Roughwall Heat-Transfer Rate on Re-Entry Nose Tips, *AIAA Paper*, **73-763**, 1973.
- [81] Simpson, R. L., A Generalized Correlation of Roughness Density Effect on the Turbulent Boundary Layer, *AIAA Journal*, **11**, pp. 242-244, 1973.
- [82] Donne, M. & Meyer, L., Turbulent Convective Heat Transfer from Rough Surfaces with Two-Dimensional Rectangular Ribs, *Int. J. Heat Mass Transfer*, **20**, pp. 583-620, 1977.
- [83] Coleman, H. W., Hodge, B. K. & Taylor, R. P., A Reevaluation of Schlichting's Surface Roughness Experiment, *J. Fluid Eng.*, **106**, pp. 60-65, 1984.
- [84] Clauser, F., The Turbulent Boundary Layer, *Advances in Applied Mechanics*, **4**, pp.1-51, 1956
- [85] Grabov, R. M. & White, C. O., Surface Roughness Effects on Nose Tip Ablation Characteristics, *AIAA Journal*, **13**, pp. 605-609, 1975.
- [86] Sigal, A. & Danberg, J. E., New Correlation of Roughness Density Effect on the Turbulent Boundary Layer, *AIAA Journal*, **25**, pp.554-556, 1990.
- [87] Kind, R. J. & Lawrysyn, M. A., Aerodynamic Characteristics of Hoar Frost Roughness, *AIAA Journal*, **30**, pp. 1703-7, 1992.
- [88] Gargaud, I. & Paumard, G., *Amelioration du transfert de chaleur par l'emploi de surfaces corruguees*, CEA-R-2464, 1964.
- [89] Draycott, A. & Lawther, K.R., Improvement of fuel element heat transfer by use of roughened surface and the application to a 7-rod cluster, *Int. Dev. Heat Transfer*, Part III, pp. 543-52, ASME, NY. 1961.
- [90] Möbius, H., Experimentelle Untersuchung des Widerstandes und der Geschwindigkeitsverteilung in Röhren mit regelmäßig angeordneten Rauigkeiten bei turbulenter Strömung, *Phys. Z.*, **41**, pp. 202-225, 1940
- [91] Chu, H. & Streeter, V.L., *Fluid flow and heat transfer in artificially roughened pipes*, Illinois Inst. of Tech. Proc., No. 4918, 1949.
- [92] Koch, R., Druckverlust und Wärmeübergang bei verwirbelter Strömung, *ForschHft. Ver. Dt. Ing.*, Series B, **24**, pp. 1-44, 1958.

- [93] Skupinski, E., *Wärmeübergang und Druckverlust bei künstlicher Verwirbelung und künstlicher Wandrauigkeiten*, Diss. Techn. Hochschule, Aachen, 1961.
- [94] Webb, R. L., Eckert, E.R.G. & Goldstein, R. J., Heat transfer and friction in tubes with repeated-rib roughness, *Int. J. Heat Mass Transfer*, **14**, pp. 601-617, 1971.
- [95] Fuerstein, G. & Rampf, G., Der Einfluß rechteckiger Rauigkeiten auf den Wärmeübergang und den Druckabfall in turbulenter Ringspaltströmung, *Wärme- und Stoffübertragung*, **2** (1), pp.19-30, 1969.
- [96] Sams, E.W., *Experimental investigation of average heat transfer and friction coefficients for air flowing in circular tubes having square-thread-type roughness*, NACA RME 52 D 17, 1952.
- [97] Fedynskii, O. S., Intensification of heat transfer to water in annular channel, *Problemi Energetiki*, *Energ. Inst. Akad. Nauk USSR*, 1959 (in Russian).
- [98] Watson, M.A.P., *The performance of a square rib type of heat transfer surface*, CEGB RD/B/N 1738, Berkeley Nuclear Laboratories, 1970.
- [99] Kjellström, B. & Larsson, A. E., *Improvement of reactor fuel element heat transfer by surface roughness*, AE-271, 1967, Data repoted by Dalle Donne & Meyer (1977).
- [100] Savage, D.W. & Myers, J.E., The effect of artificial surface roughness on heat and momentum transfer, *A.I.Ch.E.J.*, **9**, pp.694-702, 1963.
- [101] Sheriff, N., Gumley, P. & France, J., *Heat transfer characteristics of roughened surfaces*, UKAEA, TRG Report 447 (R), 1963.
- [102] Massey, F.A., *Heat transfer and flow in annuli having artificially roughened inner surfaces*, Ph. D. Thesis, University of Wisconsin, 1966.
- [103] Nunner, W., Wärmeübergang und Druckabfall in rauhen Röhren, *ForschHft. Ver. Dt. Ing.*, p. 455, 1956.
- [104] Lawn, C. J. & Hamlin, M. J., *Velocity measurements in roughened annuli*, CEGB RD/B/N 2404, Berkley Nuclear Laboratories, 1969
- [105] Stephens, M. J., *Investigations of flow in a concentric annulus with smooth outer wall and rough inner wall*, CEGB RD/B/N 1535, Berkley Nuclear Laboratories, 1970.
- [106] Perry, A.E. & Joubert, P.N., Rough-Wall Boundary Layers in Adverse Pressure Gradients, *J. Fluid Mech.*, **17**, pp.193-211, 1963.
- [107] Antonia, R.A. & Luxton, R.E., The Response of a Turbulent Boundary Layer to a Step Change in Surface Roughness, Pt. 1. Smooth to Rough, *J. Fluid Mech.*, **48**, pp. 721-762. 1971
- [108] Antonia, R.A. & Wood, D.H., Calculation of a Turbulent Boundary layer Downstream of a Step Change in Surface Roughness, *Aeronautical Quarterly*, **26**, pp. 202-210, 1975.
- [109] Pineau, F., Nguyen, V. D., Dickinson, J. & Belanger, J., Study of a Flow Over a Rough Surface with Passive Boundary-Layer Manipulators an Direct Wall Drag Measurements, *AIAA Paper*, **87-0357**, 1987.
- [110] Osaka, H. & Mochizuki, S., Mean Flow Properties of a d-type Rough Wall Boundary Layer in a Transitionally Rough and a Fully Rough Regime, *Trans. JSME ser. B*, **55**, pp. 640-647, 1989.
- [111] Byzova, N.L., Ivanov, V.N. & Garger, E.K., *Turbulence in the Atmospheric Boundary Layer*, Leningrad, Hydrometeoizdat, 1989 (in Russian).
- [112] Jackson, P.S., On the displacement height in the logarithmic wind profile. *J. Fluid Mech.*, **111**, pp. 15-25, 1981.
- [113] Wieringa, J., Updating the Davenport Roughness Clarification. *J. Wind Engineer, Industl. Aerodyn*, **41**, pp. 357-368, 1992.
- [114] Bottema, M., Parameterization of aerodynamic roughness parameters in relation with air pollutant removal efficiency of streets, *Air Pollution III, Vol.2. Air Pollution Engineering and Management*, eds. H. Power, N. Moussiopoulos & C. A. Brebbia, Comp. Mech. Publ., Southampton, pp. 235-242, 1995.